Photophysical and Structural Impact of Phosphorylated Anions Associated to Lanthanide Complexes in Water

ARTICLE *in* INORGANIC CHEMISTRY · NOVEMBER 2005

Impact Factor: 4.76 · DOI: 10.1021/ic051033o · Source: PubMed

5 AUTHORS, INCLUDING:

Loïc J Charbonnière
French National Centre for Scientific Research
116 PUBLICATIONS **2,964** CITATIONS

SEE PROFILE

Rachel Schurhammer
University of Strasbourg
46 PUBLICATIONS **974** CITATIONS

SEE PROFILE

Wipff Georges
University of Strasbourg
121 PUBLICATIONS **3,609** CITATIONS

SEE PROFILE

Inorg. Chem. **2005**, *44*, 7151–7160

Photophysical and Structural Impact of Phosphorylated Anions Associated to Lanthanide Complexes in Water

Loïc J. Charbonnière,*,† Rachel Schurhammer,‡ Samir Mameri,† Georges Wipff,*,‡ and Raymond F. Ziessel*,†

Contribution from the Laboratoire de Chimie Moléculaire, UMR CNRS 7509, ECPM-ULP, 25 rue Becquerel, 67087 Strasbourg Cedex, France, and Laboratoire MSM, Institut de Chimie, UMR CNRS 7551, Université Louis Pasteur, 4 rue Blaise Pascal, 67000 Strasbourg, France

Received June 23, 2005

A new ligand, $\mathbf{L_C}$, bis-[(6′-carboxy-2,2′-bipyridine-6-yl)]phenylphosphine oxide, in which the tridentate 6-carboxy-2,2′-bipyridyl arms are directly linked to a phenylphosphine oxide fragment, has been synthesized. The corresponding $[Ln{\cdot}\mathbf{L_C}]Cl{\cdot}xH_2O$ complexes (Ln = Eu, $x = 4$, and Tb, $x = 3$) were isolated from solutions containing equimolar amounts of $\mathbf{L_C}$ and hydrated $LnCl_3$ salts and characterized by elemental analysis, mass spectrometry, and infrared spectroscopy. The interactions of the Eu complex with various anions (AMP^{2-}, ADP^{3-}, $ATP,^{4-}$ HPO_4^{2-}, and NO_3^-) were studied by titration experiments, using UV–vis, luminescence spectroscopy, and excited-state lifetime measurements. The results are in keeping with strong interactions with the ADP^{3-}, ATP^{4-}, and phosphate anions in TRIS/HCl buffer (0.01 M, pH = 7.0), as revealed by the determination of the conditional stepwise association constants. These values are higher than the one determined for ligand $\mathbf{L_B}$, bis[(6′-carboxy-2,2′-bipyridine-6-methyl-yl)]-*n*-butylamine ($\Delta \log K \approx 1$–2). The interaction of complexes $[Ln{\cdot}\mathbf{L_B}]^+$ and $[Ln{\cdot}\mathbf{L_C}]^+$ with nitrate, monohydrogenophosphate, methyl phosphate (MeP^{2-}), methyldiphosphate ($MeDP^{3-}$), and methyltriphosphate ($MeTP^{4-}$) anions was investigated by means of quantum mechanical (QM) calculations. The results, combined with data on the photophysical impact of the sequential competitive binding of anions to the Eu complexes in water, suggest that $\mathbf{L_B}$ is too flexible to ensure a good coordination pocket, while the molecular structure of ligand $\mathbf{L_C}$ stabilizes both the formation of the lanthanide complexes and its adducts with ATP.

Introduction

Phosphates, pyrophosphates, and phosphorylated species play vital roles in a large variety of biological processes.[1] They are implicated as being *molecular batteries* in the form of di- or triphosphate nucleotides and are essential to the endoergonic phenomenon related to DNA replication. Phosphorylation reactions and hydrolysis of phosphoesters or their cyclization often induces drastic structural reorganizations essential to catalytic processes. The origin of this versatility is related to the large diversity of the $RO(PO_3)_n^{(n+1)-}$ binding modes. Its simplest member is the tetrahedral phosphate anion which in its mono- or diprotonated form, the predominant anions at physiological pH, can interact either by means of hydrogen bonding[2] both as a donor and as an acceptor or by electrostatic interactions.[3] In the latter case, the phosphate can act as (i) a monodentate ligand,[4] (ii) a bidentate ligand,[5] or (iii) a bridging unit between two[6] or three[7] metallic centers in enzymes or between two[8] or three[9] metallic centers in artificial model systems. Lengthening the phosphorylated

* To whom correspondence should be addressed. E-mail: ziessel@chimie.u-strasbg.
† Laboratoire de Chimie Moléculaire.
‡ Laboratoire MSM.

(1) Stryer, L. In *La Biochimie*, 4th ed. (in French 1997); Flammarion, Ed.; Freeman W. H. Company Publishers: New York, 1975.
(2) (a) Aoki, S.; Kimura, E. *Rev. Mol. Biotech.* **2002**, *90*, 129. (b) Beer, P. D.; Gale, P. A. *Angew. Chem., Int. Ed.* **2001**, *40*, 486.
(3) Schmidtchen, F. P.; Muller, G. *J. Chem. Soc., Chem. Commun.* **1984**, 1115.
(4) Gabricevic, M.; Anderson, D. S.; Mietzner, T. A.; Crumbliss, A. L. *Biochemistry* **2004**, *43*, 5811.
(5) Mullica, D. F.; Sappenfield, E. L.; Boatner, L. A. *Inorg. Chim. Acta* **1996**, *244*, 247.
(6) (a) Lipscomb, W. N.; Sträter, N. *Chem. Rev.* **1996**, *96*, 2375. (b) Wilcox, D. E. *Chem. Rev.* **1996**, *96*, 2435.
(7) (a) Hansen, S.; Hansen, L. K.; Hough, E. *J. Mol. Biol.* **1992**, *225*, 543. (b) Hansen, S.; Hough, E.; Svensson, L. A.; Wong, Y.-L.; Martin, S. F. *J. Mol. Biol.* **1993**, *234*, 179.
(8) (a) Ojida, A.; Mito-Oka, Y.; Dada, K.; Hamachi, I. *J. Am. Chem. Soc.* **2004**, *126*, 2454. (b) Han, M. S.; Kim, D. H. *Angew. Chem., Int. Ed.* **2002**, *41*, 20. (c) Lee, D. H.; Im, J. H.; Son, S. U.; Chung, Y. K.; Hong, J.-I. *J. Am. Chem. Soc.* **2003**, *125*, 7752.

10.1021/ic051033o CCC: $30.25
Published on Web 09/08/2005

chain adds further to the complexity by allowing the formation of macro-chelate rings.[10]

The central role of the biologically relevant phosphorylated species reveals the need for their efficient and, when possible, selective detection. Numerous analytical techniques have been applied to this sensing, such as electrochemistry,[11] absorption spectroscopy,[12] NMR spectroscopy,[13] and others,[14] but the technique of choice for sensitivity remains luminescence spectroscopy. Among the luminescence techniques used so far, conventional fluorescence appears to be the most studied,[15] but other detection method such as chemiluminescence[16] or time-resolved luminescence have also been applied. This latter technique is very attractive as it allows for very sensitive detection,[17] but it requires the use of long-lived excited-state probes. Along these lines, lanthanide complexes are of great interest, especially those of europium and terbium, whose excited-state lifetimes are in the millisecond range.[18] Lanthanide complexes also present the major advantage of being notably oxophilic and a priori positively charged, thereby providing strong electrostatic interactions with anions.[19,20] However, there still are only few lanthanide-based chemiodositometers active in pure aqueous media.[21,22]

We previously showed that the europium and terbium complexes of ligand $\mathbf{L_A}$, which both display an unsaturated coordination sphere around the lanthanide cations, can be used for the detection of anions in aprotic solvents.[20] The detection process can be understood as the result of a sequential competitive association mode where the anions partially displace the coordinated ligand with concomitant changes in the photophysical properties. Further introduction of carboxylate functions on the chromophoric bipyridyl units such as in $\mathbf{L_B}$ led to a second generation of luminescent probes efficient in water under neutral pH.[22] Complexes of $\mathbf{L_B}$ display a marked selectivity for ATP compared to the shorter phosphorylated analogues ADP and AMP. Unfortunately, these complexes remained very sensitive toward phosphate anions and suffered from weak stability at submicromolar concentrations.

In this paper, we first analyzed the structure of the $[Eu\mathbf{L_B}]^+$ complexes with different anions on the basis of quantum mechanics (QM) calculations. This led us to design and synthesize ligand $\mathbf{L_C}$ and its Eu(III) and Tb(III) complexes (Chart 1). The interaction with various phosphorylated anions is studied by UV−vis absorption and by steady-state and time-resolved luminescence spectroscopies. These studies allow us to shed some light on the structural influences of the ligand upon association to Eu(III) and on the response of the resulting complexes to anion binding.

Results and Discussion

Quantum Mechanical Studies on the Effect of Anion Binding to the $[Eu\mathbf{L_B}]^+$ Complex. From a general point of view, the formation of lanthanide complexes in solution results from the competitive interactions of the Ln^{3+} cations with the deprotonated form of ligand $\mathbf{L_B}$, counterions X^{n-}, and the surrounding solvent molecules. A key issue is to understand the mode of interaction of the resulting $[Eu\mathbf{L_B}]^+$ complex in the presence of selected anions, X^{n-}. To gain insights into the binding mode of $\mathbf{L_B}$ and to assess the contributions of its pyridino- central nitrogen atoms and the carboxylate binding sites, we first investigated the "naked" $[Eu\mathbf{L_B}]^+$ complex as such and in the presence of water molecules. In a second step, we allowed the complex to interact with mono- to tetracharged NO_3^-, HPO_4^{2-}, $MeDP^{3-}$, and $MeTP^{4-}$ anions to scrutinize the mode of coordination of the anion and the $\mathbf{L_B}$ ligand. Because of computer time

(9) Kimura, E.; Aoki, S.; Koike, T.; Shiro, M. *J. Am. Chem. Soc.* **1997**, *119*, 3068.

(10) (a) Grant, C. V.; Frydman, V.; Frydman, L. *J. Am. Chem. Soc.* **2000**, *122*, 11743. (b) Cini, R.; Burla, M. C.; Nunzi, A.; Polidori, G. P.; Zenazzi, P. F. *J. Chem. Soc., Dalton Trans.* **1984**, 2467. (c) Sigel, H.; Bianchi, E. M.; Corfù, N. A.; Kinjo, Y.; Tribolet, R.; Martin, R. B. *Chem.—Eur. J.* **2001**, *7*, 3729. (d) Bianchi, E. M.; Sajadi, S. A. A.; Song, B.; Sigel, H. *Chem.—Eur. J.* **2003**, *9*, 881.

(11) (a) Beer, P. D.; Szemes, F.; Balzani, V.; Salà, C. M.; Drew, M. G. B.; Dent, S. W.; Maestri, M. *J. Am. Chem. Soc.* **1997**, *119*, 11864. (b) Albeda, M. T.; Bernardo, M. A.; Garcia-Espaòa, E.; Godino-Salido, M. L.; Luis, S. V.; Melo, M. J.; Pina, F.; Soriano, C. *J. Chem. Soc., Perkin Trans. 2* **1999**, 2545. (c) Ruiz, J.; Medel, M. J. R.; Daniel, M.-C.; Blais, J.-C.; Astruc, D. *Chem. Commun.* **2003**, 464.

(12) (a) Tobey, S. L.; Jones, B. D.; Anslyn, E. V. *J. Am. Chem. Soc.* **2003**, *125*, 4026. (b) Sancenon, F.; Descalzo, A. B.; Martinez-Máòez, R.; Miranda, M. A.; Soto, J. *Angew. Chem., Int. Ed.* **2001**, *40*, 2640. (c) McCleskey, S. C.; Griffin, M. J.; Schneider, S. E.; McDevitt, J. T.; Anslyn, E. V. *J. Am. Chem. Soc.* **2003**, *125*, 1114. (d) Morey, J.; Orell, M.; Barcelo, M. A.; Deya, P. M.; Costa, A.; Ballester, P. *Tetrahedron Lett.* **2004**, *45*, 1261. (e) Tamiaki, H.; Unno, S.; Takeuchi, E.; Tameshige, N.; Shinoda, S.; Tsukube, H. *Tetrahedron* **2003**, *59*, 10477. (f) Govenlock, L. J.; Mathieu, C. E.; Maupin, C. L.; Parker, D.; Riehl, J. P.; Siligardi, G.; Williams, J. A. G. *Chem. Commun.* **1999**, 1699.

(13) (a) Hosseini, M. W.; Blacker, A. J.; Lehn, J.-M. *J. Am. Chem. Soc.* **1990**, *112*, 3896. (b) Hosseini, M. W.; Lehn, J.-M.; Mertes, M. P. *Helv. Chim. Acta* **1983**, *66*, 2454.

(14) Sazani, P.; Larralde, R.; Szostak, J. W. *J. Am. Chem. Soc.* **2004**, *126*, 8370.

(15) (a) Vance, D. H.; Czarnik, A. W. *J. Am. Chem. Soc.* **1994**, *116*, 9397. (b) Schneider, S. E.; O'Neil, S. N.; Anslyn, E. V. *J. Am. Chem. Soc.* **2000**, *122*, 542. (c) Padilla-Tosta, M. E.; Lloris, J. M.; Martinez-Maòez, R.; Pardo, T.; Sancenon, F.; Soto, J.; Marcos, M. D. *Eur. J. Inorg. Chem.* **2001**, 1221. (d) Stojanovic, M. N.; de Prada, P.; Landry, D. W. *J. Am. Chem. Soc.* **2000**, *122*, 11547. (e) Mizukami, S.; Nagano, T.; Urano, Y.; Odani, A.; Kikuchi, K. *J. Am. Chem. Soc.* **2002**, *124*, 3920. (f) Kanekiyo, Y.; Naganawa, R.; Tao, H. *Chem. Commun.* **2004**, 1006. (g) Chen, C.-A.; Yeh, R.-H.; Lawrence, D. S. *J. Am. Chem. Soc.* **2002**, *124*, 3840.

(16) Cruz-Aguado, J. A.; Chen, Y.; Zhang, Z.; Elowe, N. H.; Brook, M. A.; Brennan, J. D. *J. Am. Chem. Soc.* **2004**, *126*, 6878.

(17) Hemmilä, I.; Harju, R. In *Bioanalytical Applications of Labeling Technologies*; Hemmilä, I., Ståhlberg, T., Mottram, P., Eds.; Walac Oy and EG&G Cie: Turku, Finland, 1995; Chapter 5, p 83.

(18) (a) Bünzli, J.-C. G. In *Lanthanide Probes in Life, Chemical and Life Sciences*; Bünzli, J.-C. G., Choppin, G. R., Eds.; Elsevier: Amsterdam, 1989; p 228. (b) Charbonnière, L. J.; Guardigli, M.; Cesario, M.; Roda, A.; Sabbatini, N.; Ziessel, R. *J. Am. Chem. Soc.* **2001**, *123*, 2436. (c) Petoud, S.; Cohen, S. M.; Bünzli, J.-C. G.; Raymond, K. N. *J. Am. Chem. Soc.* **2003**, *125*, 13324.

(19) (a) Tsukube, H.; Shinoda, S. *Chem. Rev.* **2002**, *102*, 2389. (b) Yamada, T.; Shinoda, S.; Tsukube, H. *Chem. Commun.* **2002**, 1218. (c) Tsukube, H.; Yamada, T.; Shinoda, S. J. *Alloys Compd.* **2004**, *374*, 40. (d) Best, M. D.; Anslyn, E. V. *Chem.—Eur. J.* **2003**, *9*, 51.

(20) Montalti, M.; Prodi, L.; Zaccheroni, N.; Charbonnière, L. J.; Douce, L.; Ziessel, R. *J. Am. Chem. Soc.* **2001**, *123*, 12694. (b) Charbonnière, L. J.; Ziessel, R.; Montalti, M.; Prodi, L.; Zaccheroni, N.; Boehme, C.; Wipff, G. *J. Am. Chem. Soc.* **2002**, *124*, 7779.

(21) (a) Parker, D. *Coord. Chem. Rev.* **2000**, *205*, 109. (b) Reany, O.; Gunnlaugsson, T.; Parker, D. *Chem. Commun.* **2000**, 473. (c) Bretonnière, Y.; Cann, M. J.; Parker, D.; Slater, R. *Chem. Commun.* **2002**, 1930. (d) Bretonnière, Y.; Cann, M. J.; Parker, D.; Slater, R. *Org. Biomol. Chem.* **2004**, *2*, 1624.

(22) Mameri, S.; Charbonnière, L. J.; Ziessel, R. F. *Inorg. Chem.* **2004**, *43*, 1819.

Chart 1

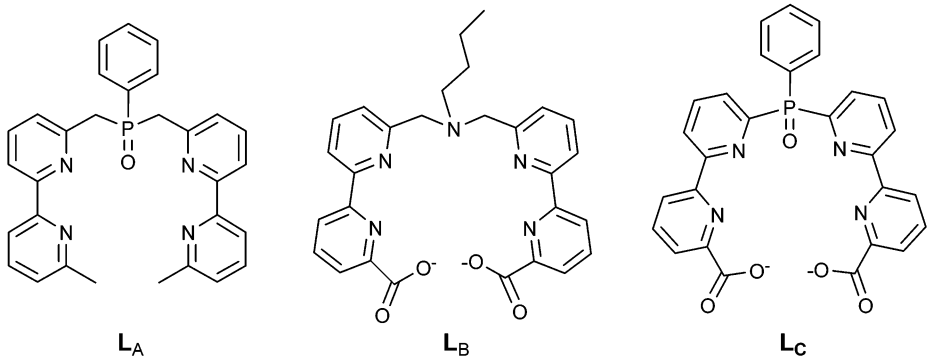

limitations, the butyl chain of $\mathbf{L_B}$ was replaced with a methyl group and ADP^{3-} and ATP^{4-} were mimicked by their methyl analogues, $MeDP^{3-}$ and $MeTP,^{4-}$ assuming that they bind similarly to the complex. Furthermore, the effect of water coordination was studied in the $[Eu\mathbf{L_B}(H_2O)_2]^+$ and $[Eu\mathbf{L_B}(HPO_4)(H_2O)_2]^-$ complexes. Insights into the electron distribution are obtained from the Mulliken charges.

Figures 1 and S1 (Supporting Information) show the optimized structures of the complexes, and the main optimized distances between europium and X^{n-} or the oxygen or nitrogen atoms of $\mathbf{L_B}$ are given in Table 1 and shown in Figure S2 (Supporting Information). The central tertiary amine was numbered N_1, the two adjacent N_{pyr} atoms were labeled N_2 and N_4, and the corresponding neighboring N_{pyr} atoms were N_3 and N_5 (Scheme 1). The calculated distances

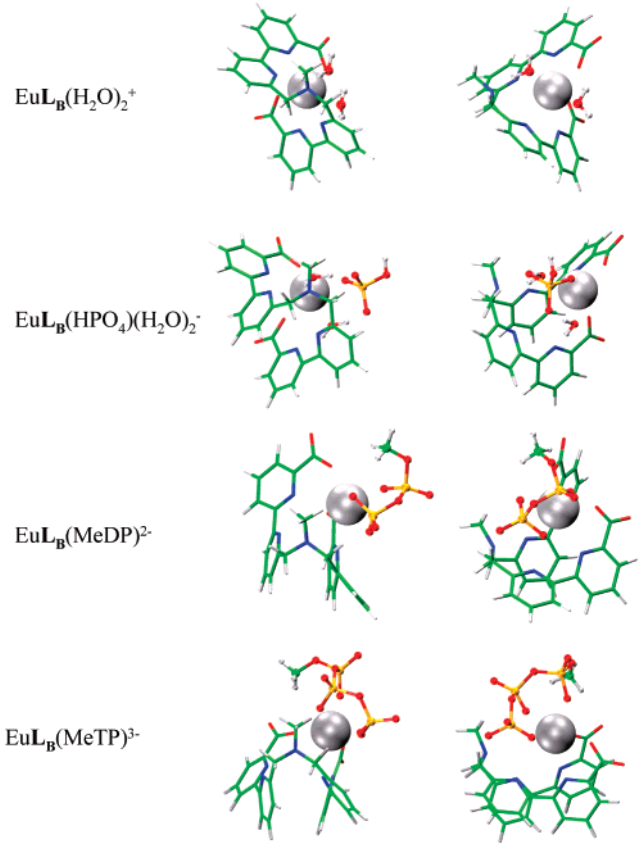

Figure 1. Orthogonal views of the QM-optimized $[Eu\mathbf{L_B}]^+$ complexes with water, HPO_4^{2-}/water, $MeDP^{3-}$, and $MeTP^{4-}$.

demonstrate the versatile character of the coordination of the $\mathbf{L_B}$ ligand to the cation, depending on the charge and topology of the added anion and on the coordinaion of water molecules. As expected, the metal ensures its coordination to two hard carboxylate oxygens of the ligand ($Eu-O_L$ distances range from 2.2 to 2.7 Å) to the detriment of the softer central N_1 and N_{pyr} nitrogen atoms. These $Eu-O_L$ distances are in keeping with those found in X-ray structures of a podand-type ligand[18b] or a calix[4]arene-preorganized platform.[23]

In the absence of competing anions or water molecules, $\mathbf{L_B}$ forms an $[Eu\mathbf{L_B}]^+$ complex of approximate *Cs* symmetry (Figure S1, Supporting Information), in which the metal coordinates to all binding sites. The two carboxylate oxygen atoms (at 2.2 Å), the four N_{bipy} (2.5 to 2.7 Å), and the apical nitrogen (2.8 Å) lead to an important charge reduction on europium ($q_{Eu} = 1.52$ e). Co-complexation of two H_2O molecules is however sufficient to disrupt the coordination of N1 (3.8 Å) and to increase the distance with N_4 to 3.0 Å, while the other bonds vary by only ≈ 0.1 Å (Figure 1). The coordination of the NO_3^- anion leads to a more asymmetrical $[Eu\mathbf{L_B}(NO_3)]$ complex which displays elongated $Eu-N_1$ and $Eu-N_5$ "bonds" (2.9 Å) and a somewhat shorter Eu−N4 bonds (2.3 Å). The NO_3^- anion is bound in a bidentate mode as found in related europium−nitrate complexes[24] (Figure S1). We observe the nonequivalence of the two $Eu-O_L$ distances (2.7 and 2.3 Å), which bracket the $Eu-O_{NO_3}$ distance (2.5 Å).

The HPO_4^{2-} anion which binds in a bidentate fashion to the metal (at 2.6 and 2.8 Å) is sterically more demanding than NO_3^- and more negatively charged; therefore, it induces more charge transfer to the metal and weakens the other metal−ligand bonds (Figure S1). Thus, in the $[Eu\mathbf{L_B}(HPO_4)]^-$ complex, one bipy arm retains loose contact with Eu^{3+} (2.6 and 2.8 Å), while the second N_{bipy} (4.0 and 4.7 Å) and N_1 (3.9 Å) atoms are shifted away, thus preventing orbital overlap with europium. The addition of two H_2O molecules

(23) Ziessel, R. F.; Charbonnière, L. J.; Cesario, M.; Prangé, T.; Guardigli, M.; Roda, A.; van Dorsselaer, A.; Nierengarten, H. *Supramolecular Chemistry* **2003**, *15*, 277.
(24) (a) Bünzli, J.-C. G.; Klein, B.; Wesner, D.; Alcock, N. W. *Inorg. Chim. Acta* **1982**, *59*, 269. (b) Bünzli, J.-C. G.; Klein, B.; Chapuis, G.; Schenk, K. J. *Inorg. Chem.* **1982**, *21*, 808. (c) Bünzli, J.-C. G.; Leonard, G. A.; Plancherel, D.; Chapuis, G. *Helv. Chim. Acta* **1986**, *69*, 288.

Table 1. Eu−O and Eu−N Distances of the QM-Optimized $[Eu\mathbf{L_B}]^+$ Complex and Its Adducts

		$Eu\mathbf{L_B}^+$	$Eu\mathbf{L_B}(H_2O)_2^+$	$Eu\mathbf{L_B}NO_3$	$Eu\mathbf{L_B}(HPO_4)^-$	$Eu\mathbf{L_B}(HPO_4)\,(H_2O)_2^-$	$Eu\mathbf{L_B}MeDP^{2-}$	$Eu\mathbf{L_B}MeTP^{3-}$
$\mathbf{L_B}$	N_1	2.762	3.806	2.901	3.891	4.849	4.489	4.873
	N_2	2.693	2.760	2.779	2.821	4.078	3.834	3.641
	N_3	2.554	2.542	2.663	2.589	2.790	3.038	2.801
	N_4	2.558	3.043	2.274	4.690	4.599	4.281	5.456
	N_5	2.518	2.509	2.897	4.025	3.841	3.167	4.344
	O_1	2.244	2.279	2.731	2.306	2.273	2.383	2.371
	O_2	2.199	2.248	2.303	2.286	2.316	2.353	2.346
H_2O	O_{w1}		2.458			2.322		
	O_{w2}		2.453			2.426		
HPO_4^{2-}	O_{P1}				2.241	2.240	2.334	2.287
	O_{P2}				2.312	3.836	2.357	2.288
	O_{P3}				4.168	3.854	2.247	2.335
NO_3^-	O_{N1}			2.484				
	O_{N2}			2.512				
	O_{N3}			4.149				

Scheme 1

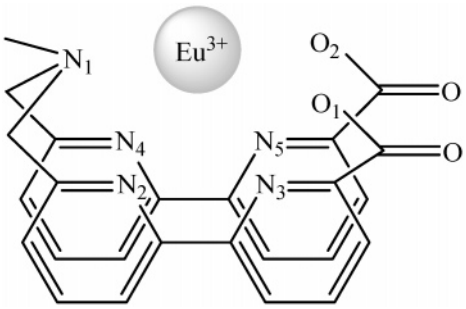

leads to the $[Eu\mathbf{L_B}(HPO_4)(H_2O)_2]^-$ complex (Figure 1), in which the strong water coordination (at 2.3 to 2.4 Å) induces a change in the binding mode of HPO_4^{2-}, which becomes monodentate (at 2.2 Å), as in the solid-state structure of the zircon−lanthanide orthophosphate complexes.[25] The metal sits on the carboxylate side of $\mathbf{L_B}$ making loose contacts with the nearest N_{bipy} nitrogens (2.8 and 3.8 Å) and being more remote from the other N_2 and N_4 nitrogen atoms (4.1 and 4.6 Å) and from N_1 (4.8 Å).

The evolution of the complexes with monohydrogenophosphate, HPO_4^{2-}, methyl-diphosphate, $MeDP^{3-}$, and methyl-triphosphate, $MeTP^{4-}$ (Figure 1), shows a progressive decomplexation of the nitrogen binding sites of the $\mathbf{L_B}$ ligand, which remains anchored via its carboxylate oxygens. $MeDP^{3-}$ is coordinated via 2 + 1 phosphoryl oxygen atoms (at ≈ 2.3 Å): two from the terminal PO_3^{2-} moiety and one from the $PO_2(OMe)^-$ phosphate, forming six-membered chelate rings. The nearest nitrogen atoms are N_3 and N_5 (at 3.0 and 3.2 Å), whereas N_2 and N_4 are still more remote (3.8 and 4.3 Å). In the $[Eu(\mathbf{L_B})MeTP]^{3-}$ complex, the $MeTP^{4-}$ anion is coordinated via the three phosphate groups, achieving a tris-monodentate 1 + 1 + 1 coordination. A similar binding mode is found in the X-ray structures of the, e.g., $[Cd(HATP)_2]$,[4−] [26] $[Mg(HATP)_2]^{4-}$, or $[Ca(HATP)_2]^{4-}$ ions.[27] As a result, only one bipy arm of $\mathbf{L_B}$ remains coordinated to the metal (via one Nbipy nitrogen atom).

In all complexes, there is significant electron transfer to europium, whose charge (in e) decreases with the charge of the added counterions from 1.52 (in $[Eu\mathbf{L_B}]^+$) to 1.39 in the NO_3^- adduct, 1.16 in the HPO_4^{2-} adduct, 1.07 in the $MeDP^{3-}$ adduct, and 1.01 in the $MeTP^{4-}$ adduct, thus reducing the metal affinity for ligand $\mathbf{L_B}$.

Two main points can be deduced from these QM calculations. First, all examples show that the first coordinating atom of $\mathbf{L_B}$ to be displaced upon anion binding is the central N_1 atom. Increasing the anionic interaction gradually leads to the lengthening of the Eu−N_2 (or Eu−N_4) distances followed by that of Eu−N_3 (or Eu−N_5), whereas the coordination of the ligand is then mainly achieved by the carboxylate functions. Using the lengthening of the Eu−N distances as a tool to gauge the degree of decomplexation of $\mathbf{L_B}$, we observed the following sequence: $NO_3^- \ll MeDP^{3-} < HPO_4^{2-}\cdot 2H_2O < MeTP^{4-}$. This is also the sequence of the increasing interactions of the anion with the complex. These results are in excellent agreement with those found on the effect of these anions on the photophysical properties of the $[Eu\mathbf{L_B}]^+$ complex in water.[22] When the anion competition becomes strong enough, as observed with HPO_4^{2-} or ATP^{4-} in water, a ternary species formed in which the coordination of one of the bipyridyl arms is weakened, resulting in an hypsochromic shift in the absorption spectra and a decrease of the luminescence intensity caused by decreased excitation efficiency.

In light of these results, it is expected that a reinforcement of the lanthanide to ligand coordination should decrease the interaction with the incoming anion, leading to a selectivity toward the strongest binder of the studied series, $ATP.^{4-}$ Assuming that the weak side of $\mathbf{L_B}$ is the central N_1 atom, we decided to strengthen the coordination by introducing a phenylphosphine function, as in the newly synthesized ligand $\mathbf{L_C}$. QM calculations indeed confirm that PO strongly binds to the lanthanide cations.[28] To reduce the conformational freedom, the bipyridyl arms were directly linked to the phosphorus atom, leading to two fused five-membered chelate rings upon lanthanide coordination (Chart 2).

(25) Mullica, D. F.; Sappenfield, E. L.; Boatner, L. A. *Inorg. Chim. Acta* **1996**, *244*, 247.
(26) Cini, R.; Marzilli, L. G. *Inorg. Chem.* **1988**, *27*, 1855.
(27) Cini, R.; Burla, M. C.; Nunzi, A.; Polidori, G. P.; Zenazzi, P. F. *J. Chem. Soc., Dalton Trans.* **1984**, 2467.
(28) Baaden, M.; Berny, F.; Boehme, C.; Muzet, N.; Schurhammer, R.; Wipff, G. *J. Alloys Compd.* **2000**, *303*, 104.

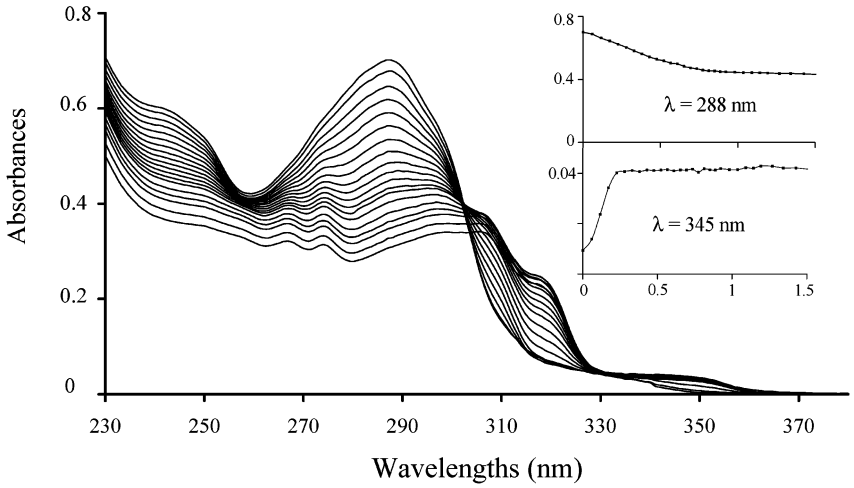

Figure 2. Evolution of the UV−vis absorption spectra of $\mathbf{L_C}$ upon addition of $EuCl_3 \cdot 6H_2O$ in water (0.01 M TRIS/ HCl buffer, pH 7.0) The inset shows the evolution of the optical densities at 288 and 345 nm as a function of the [Eu]/[$\mathbf{L_C}$] ratio after correction for dilution.

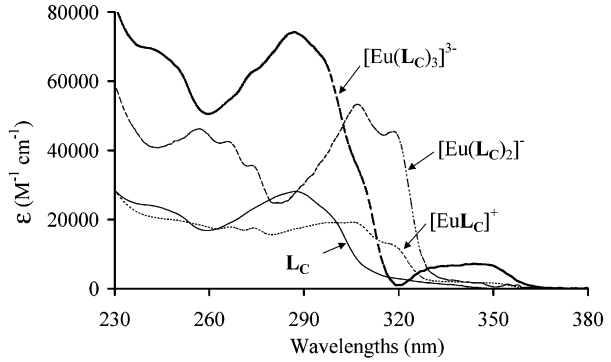

Figure 3. Calculated UV-vis absorption spectra of the species formed upon titration of $\mathbf{L_C}$ with $EuCl_3.6H_2O$ in water (pH 7.0, 0.01 M TRIS/ HCl).

Chart 2. Schematic Coordination Modes of Ligands $\mathbf{L_B}$ (left) and $\mathbf{L_C}$ (right)

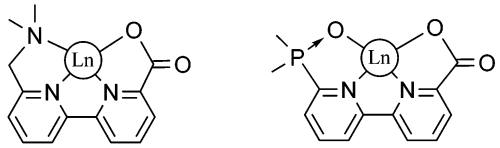

Coordination Behavior of $\mathbf{L_C}$ with Europium in Solution. The complexation of lanthanide cations by $\mathbf{L_C}$ was first studied by UV−vis spectrophotometric titration experiments. The spectrum of $\mathbf{L_C}$ was monitored as a function of the aliquots of $EuCl_3 \cdot 6H_2O$ in water solutions, containing 0.01 M TRIS buffered at pH 7.0 either by HCl or $HClO_4$.

In a TRIS/HCl buffer, the addition of europium to $\mathbf{L_C}$ first resulted in the appearance of a new absorption band in the 340−360 nm region (Figure 2). Interestingly, the increase in the optical density in this region reaches a maximum around 0.33 equiv of europium (see inset in Figure 3), strongly indicating the presence of an [Eu($\mathbf{L_C}$)$_3$] species. During the titration, the maximum absorption of the $\pi-\pi^*$ transitions on the ligand gradually decreases in intensity (taking dilution effects into account) and shifts from 287 nm in absence of europium to 305 nm at the end of the titration. The titration was then analyzed using a factorial analysis

Table 2. Cumulative Conditional Stability Constants for Equilibria 1−3 in Water at pH 7.0, 0.01 M TRIS/HCl or $HClO_4$ for Ligands $\mathbf{L_B}$ and $\mathbf{L_C}$

constants	$\mathbf{L_C}/Eu^{3+}$ TRIS/HCl	$\mathbf{L_C}/Eu^{3+}$ TRIS/$HClO_4$	$\mathbf{L_B}/Eu^{3+}$ TRIS/$HClO_4$[22]
$\log \beta_{11}$	6.3 ± 0.3	7.0 ± 0.8	5.7 ± 0.4
$\log \beta_{12}$	11.8 ± 0.3	13.0 ± 1.1	10.4 ± 1.0
$\log \beta_{13}$	18.1 ± 0.4	−	−

and fitted to eqs 1−3 using the nonlinear least-squares algorithm implemented in the SpecFit software[29]

$$Eu + \mathbf{L_C} \leftrightarrows [Eu\mathbf{L_C}]^+ \quad \beta_{11} = \frac{[Eu\mathbf{L_C}]}{[Eu][\mathbf{L_C}]} \tag{1}$$

$$Eu + 2\mathbf{L_C} \leftrightarrows [Eu(\mathbf{L_C})_2]^- \quad \beta_{12} = \frac{[Eu(\mathbf{L_C})_2]}{[Eu][\mathbf{L_C}]^2} \tag{2}$$

$$Eu + 3\mathbf{L_C} \leftrightarrows [Eu(\mathbf{L_C})_3]^{3-} \quad \beta_{13} = \frac{[Eu(\mathbf{L_C})_3]}{[Eu][\mathbf{L_C}]^3} \tag{3}$$

The conditional cumulative association constants are gathered in Table 2. The resulting calculated UV−vis absorption spectra of the different species and the evolution of their concentrations are presented for TRIS/HCl in Figures 3 and S3 (Supporting Information), respectively.

These spectra are particularly informative for the coordination behavior of the ligand in the [Eu($\mathbf{L_C}$)$_3$]$^{3-}$ complex. The maximum of absorption for the $\pi-\pi^*$ transitions centered on the bipyridyl (bipy) moieties is at the same wavelength for this complex as for the free ligand ($\lambda = 288$ nm). This clearly indicates that there is no trans to cis isomerization in the bipy unit, as is observed when this part of the molecule is protonated[30] or chelated to a metal.[31] The

(29) (a) Gampp, H.; Maeder, M.; Meyer, C. J.; Züberbühler, A. D. *Talanta* **1986**, *33*, 943. (b) Gampp, H.; Maeder, M.; Meyer, C.; Züberbühler, A. D. *Talanta* **1985**, *32*, 257.
(30) (a) Westheimer, F. H.; Benfey, O. T. *J. Am. Chem. Soc.* **1956**, *78*, 5309. (b) Nakamoto, K. *J. Phys. Chem.* **1960**, *64*, 1420. (c) Krumholz, P. *J. Am. Chem. Soc.* **1951**, *73*, 3487.
(31) Comby, S.; Imbert, D.; Chauvin, A.-S.; Bünzli, J.-C. G.; Charbonnière, L. J.; Ziessel, R. *Inorg. Chem.* **2004**, *43*, 7369.

spectrum also displays a new absorption band spanning from 320 to 360 nm, with an average absorption coefficient of 2400 M^{-1} cm^{-1} per ligand unit (ϵ = 7200 M^{-1} cm^{-1} at 344 nm). Because of the intensity of the band, its position in the spectrum, and its similarity with the one observed with the Eu complex of ligand $\mathbf{L_A}$,[20b] this transition was ascribed to an n → p* transition centered on the phenylphosphine oxide moiety. All of these observations suggest that the coordination of $\mathbf{L_C}$ in the [M($\mathbf{L_C}$)$_3$] species mainly occurs via the phosphine oxide oxygen atom and that the bipyridyl units are not directly coordinated to the cation. The spectra of [Eu($\mathbf{L_C}$)$_2$]$^-$ and [Eu$\mathbf{L_C}$]$^+$ also have absorbances in the 350 nm region, but the main absorption band of the bipy is now shifted to lower energies (around 306 nm), in keeping with the chelation of the bipy units.[31]

The situation is very different in a TRIS/$HClO_4$ buffer (Figures S4−S6, Supporting Information). The low-energy absorption band attributed to the n → p* transition centered on the phenylphosphine oxide moiety is much weaker here. Full treatment of the data showed the formation of only two new species, the [Eu$\mathbf{L_C}$]$^+$ and [Eu($\mathbf{L_C}$)$_2$]$^-$ complexes. Their related conditional association constants are higher than those calculated in the TRIS/HCl buffer (Table 1). The different behaviors associated with an increased stability with perchlorate salts clearly indicate that the salt plays an important role in the complexation. It is expected that chloride anions will interact more strongly with europium than the softer perchlorates. The interaction of the latter being weaker, the density of charge on the cation remains significant, and the coordination of $\mathbf{L_C}$ via both the PO and bipy moieties is strengthened. Conversely, with the coordinated chloride anions, the charge density on the cation is decreased and the electrostatic interaction of the carboxylate function of the ligand becomes weaker, at the benefit of the dipolar interactions with the PO moieties. An interesting consequence is that the coordination of the softer PO moiety of $\mathbf{L_C}$ is favored, as observed in the [Eu($\mathbf{L_C}$)$_3$]$^{3-}$ complex.

Synthesis of the Eu(III) and Tb(III) Complexes and Interaction with Anions. The europium complex of $\mathbf{L_C}$ was obtained by mixing equimolar amounts of the ligand and $EuCl_3 \cdot 6H_2O$ salts in a MeOH/water mixture, followed by neutralization with Et_3N and precipitation with Et_2O. Elemental analysis of the complex revealed a structure containing one europium and one chloride atom per ligand together with four water molecules. The one to one stoichiometry was further confirmed by FAB/MS with the major peak corresponding to the [Eu$\mathbf{L_C}$]$^+$ species at 671.1 and 673.1 *m*/*z* units having the expected isotopic pattern of the ^{151}Eu and ^{153}Eu isotopes. The IR spectrum of the complex displays intense absorption bands around 1625 cm^{-1} attributed to stretching vibrations of the C═O bond of the coordinated carboxylate groups,[32] which are found at higher energy (1717 cm^{-1}) in the protonated carboxylic acid form of the free ligand. The characteristic P═O absorption band, observed around 1200 cm^{-1} in substituted phenylphosphine oxides,[33] appears at 1238 cm^{-1} in $\mathbf{L_C}$ and is shifted toward lower energies in the complexes (1186 and 1187 cm^{-1}, respectively, for Eu and Tb).

Table 3. Photophysical Data for [Ln$\mathbf{L_C}$]$^+$ Complexes (Ln = Eu and Tb) in Water

	$\mathbf{L_C}$		$\mathbf{L_B}$	
	Eu	Tb	Eu	Tb
	absorption			
λ_{max} (nm)	308	308	307	308
ϵ (M^{-1} cm^{-1})	23700	24000	18000	18150
	emission			
λ_{max} (nm)	615[a]	545[b]	620[a]	545[b]
Φ_{H_2O} (%)[c]	5.3	8.7	4.6	0.4
Φ_{D_2O} (%)[c]	11.8	12.3		
τ_{H_2O}	0.35	0.84	0.36	0.78
τ_{D_2O}	2.24	1.39	1.75	1.15
q[d,e]	2.6 (2.1)	2.0	2.3	1.8
τ_{TRIS}[f]	0.35 (50%)		0.34 (58%)	
	0.74 (50%)		1.11 (42%)	
τ_{TRIS/D_2O}[g]	1.9		0.82	
			1.44	
q_{TRIS}[d,e]	0.7 (0.6)		0 (0)	
	2.5 (2.2)		1.7 (1.8)	

[a] $^5D_0$ → $^7F_2$ transition centered on europium. [b] $^5D_4$ → $^7F_5$ transition centered on terbium. [c] Relative estimated error ±15%. [d] Calculated according to ref 34 with $q_{Eu} = 1.2(\Delta k - 0.25)$ and $q_{Tb} = 5.0(\Delta k - 0.06)$, where $\Delta k = 1/\tau_{H_2O} - 1/\tau_{D_2O}$; estimated error ±0.3 water molecules. [e] Calculated according to ref 35 with $q_{Eu} = 1.1(\Delta k - 0.31)$; estimated error ±0.3 water molecules. [f] Measured in 0.01 M TRIS/HCl buffered solution at pH 7.0 in water. [g] Obtained by the evaporation of water and replacement by D_2O.

The UV−vis absorption spectra of the complexes confirmed the results obtained by the previous set of titration experiments, showing the intense absorption band at 308 nm corresponding to the $\pi \rightarrow \pi^*$ transitions centered on the bipyridyl units (Table 3), together with a broad band of medium intensity ($\epsilon \approx 2800$ cm^{-1}) around 345 nm, which we attributed to phosphine oxide-centered n → π^* transitions.

Upon excitation in the $\pi \rightarrow \pi^*$ absorption bands, the complexes display the characteristic emission spectra of lanthanide complexes, dominated by the $^5D_X \rightarrow {}^7F_Y$ ($X = 0$ for Eu, 4 for Tb; $Y = 0-6$) electronic transitions of the lanthanide cations.[18] The luminescence quantum yields were determined both in water and deuterated water and showed both complexes to be luminescent in aqueous solutions. Lanthanide-based luminescence lifetimes, τ, were also determined in both solvents, which allowed us to infer the number of water molecules coordinated to the cations.[34,35] For both complexes, a hydration number of two was calculated. If one assumes a total coordination number of nine, this is in accordance with a heptadentate binding mode of the ligand: the two carboxylate functions, the four nitrogen atoms of the bipyridyl moieties, and the phosphine oxide oxygen atom. Particularly interesting data resulted from the luminescence lifetime measurements in buffered solutions of TRIS/HCl at pH 7.0, for which the decay became biexponential.

(32) Silverstein, R. M.; Bassler, G. C. *Identification Spectrométriques des Composés Organiques*; Gauthier-Villars: Paris, 1968.

(33) Martin, K. A.; Horwitz, E. P.; Ferraro, J. R. *Solv. Ext. And Ion Exch.* **1986**, *4*, 1149.

(34) Beeby, A.; Clarkson, I. M.; Dickins, R. S.; Faulkner, S.; Parker, D.; Royle, L.; de Sousa, A. S.; Williams, J. A. G.; Woods, M. *J. Chem. Soc., Perkin Trans. 2* **1999**, 493.

(35) Supkowski, R. M.; Horrocks, W. DeW., Jr. *Inorg. Chim. Acta* **2002**, *340*, 44.

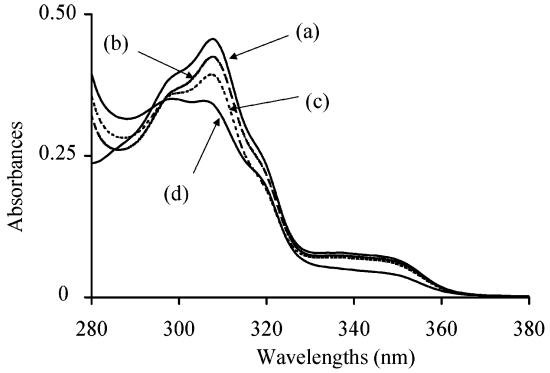

Figure 4. UV-vis absorption spectra of a solution of $[Eu\mathbf{L_C}]^+$ containing 2 equiv of (a) NO_3^-, (b) AMP^{2-}, (c) ADP^{3-}, and (d) ATP^{4-} in water (0.01 M TRSI/HCl, pH 7.0).

A good fit was then obtained with two species of approximately the same population according to pre-exponential factors with lifetimes of 740 and 350 μs. The latter value is very close to the one measured in nonbuffered water. Replacing H_2O with D_2O in the same buffer restored a monoexponential behavior with a 1900 μs lifetime. These values point to environments of the two species being composed of respectively two and one water molecules in the first coordination sphere, for the short- and long-lived species, and show that the TRIS/HCl buffering medium is likely to provide a coordinated chloride anion. For the sake of comparison, the same study was done on the europium complex of ligand $\mathbf{L_B}$. The same behavior was observed except that the two species were found to contain, respectively, no and two water molecules.

The interactions of different anionic species with the complex were then studied by titration experiments in which increasing quantities of anions were added to solutions of the complex in buffered 0.01 M TRIS/HCl solutions at pH 7.0. The complexation of NO_3^-, AMP^{2-}, ADP^{3-}, ATP^{4-}, and HPO_4^{2-} was monitored by a combination of UV−vis absorption spectroscopy, steady-state emission spectroscopy, and europium-based luminescence lifetime measurements. The results were fitted according to eq 4

$$[Eu\mathbf{L_C}]^+ + X^{n-} \leftrightarrows [Eu\mathbf{L_C}X]^{(n-1)-} \quad K_{111} = \frac{[Eu\mathbf{L_C}X]}{[Eu\mathbf{L_C}][X]} \quad (4)$$

where K_{111} represents the conditional association constant for the coordination of X^{n-}.

The addition of nitrate or AMP^{2-} anions did not lead to any significant change in absorption or emission spectra, indicating that their interactions are very weak. The addition of ADP^{3-} resulted in little changes in the UV−vis absorption spectra (Figures 4 and S7−S9, Supporting Information). However, the evolution of the emission spectra showed only a small increase in the luminescence intensity, but the interaction was unambiguously revealed by a more than 20% increase in the luminescence lifetime of the europium complex (Table T2, Supporting Information). The addition of ATP^{4-} led to clearer changes in the UV−vis absorption spectra with a marked decrease of the absorption bands at 308 nm and at around 345 nm (Figures S10−S12 and Table T3, Supporting Information). Titration with HPO_4^{2-} resulted in a similar behavior to that observed with ATP^{4-} (Figures S13−S15). The conditional stability constants obtained by UV−vis absorption spectroscopy are gathered in Table 4.

Table 4. Conditional Stability Constants[a] for the Association of Various Anions to the Europium Complex of $\mathbf{L_C}$ According to Eq 4 (in water TRIS/HCl 0.01 M, pH 7.0)

X^-		NO_3^-	AMP^{2-}	ADP^{3-}	ATP^{4-}	HPO_4^{2-}
$\mathbf{L_C}$	$\log K_{111}$	−[b]	−[b]	5.5 ± 0.2	5.5 ± 0.2	5.2 ± 0.3
$\mathbf{L_B}$[c]	$\log K_{111}$	−[b]	−[b]	−[b]	4.3 ± 0.2	4.4 ± 0.1

[a] Obtained by UV−vis absorption spectroscopy as the average value of at least two distinct titrations. [b] Too weak to be measured by UV−vis spectroscopy ($\log K_{111} < 3.3$). [c] Aqueous TRIS/$HClO_4$ 0.01 M, corrected for possible protonation of the anion at pH 7.0 (see Experimental Section).

The evolution of the emission intensity and luminescence lifetimes is very similar for ADP^{3-}, ATP^{4-}, and HPO_4^{2-}, showing a small increase of the emission and a 20 to 30% increase of the lifetimes at the end of the titrations (Figures S16). This behavior can be simply interpreted by the complexation of these anions in the first coordination sphere of europium, thereby increasing the luminescence lifetime. In contrast to the small decrease of the absorption in the $\pi \rightarrow \pi^*$ region, the small increase in luminescence intensity upon excitation at 300 nm is to be associated with an improvement of the overall quantum efficiency in the ternary species formed. This is mainly the result of the lowering of nonradiative deactivation pathways related to the removal of the OH oscillators of water molecules.

The conditional stepwise association constants for the formation of the ternary species, K_{111}, show that the selectivity previously observed for ATP^{4-} compared to ADP^{3-} with the complexes of ligand $\mathbf{L_B}$ is totally lost with $\mathbf{L_C}$. When the anion is able to associate to the $[Eu\mathbf{L_C}]^+$ complex, as do HPO_4^{2-}, ADP^{3-}, and ATP^{4-}, the association is strong. The different behaviors observed for the two dianionic species, AMP^{2-} and HPO_4^{2-}, can be explained by steric constraints resulting from the bulky adenine-ribose substituent of the phosphate in AMP and the higher basicity of the mono-hydrogenophosphate anion ($pK_3(AMPH_3^+) = 6.21$,[10d] $pK_2(H_3PO_4) = 7.2$ [37]). It is also not surprising that AMP does not interact whereas ADP does, as it is well established that the ADP interaction with cationic species of group II or transition elements of the first series[10d] is stronger by 1−2 orders of magnitude. In the case of ADP and ATP, the higher charge combined to the removal of the adenine-ribose residue again allows for a stronger association with $[Eu\mathbf{L_C}]^+$.

Quantum Mechanical Studies on the Effect of Anion Binding to the $[Eu\mathbf{L_C}]^+$ Complex. Insights into the structural consequences of the interaction of the HPO_4^{2-} and $MeTP^{4-}$ anions with $[Eu\mathbf{L_C}]^+$ were obtained by QM modeling. Figure 5 presents views of the resulting ternary

(36) *Handbook of Chemistry and Physics*, 54th ed.; Weast, R. C., Ed.; CRC Press: Cleveland, OH, 1974.
(37) Tabulated $pK_2(H_3PO_4)$ values of the literature vary from 6.63 (at a 0.1 M fixed ionic strengh) to 7.21, see: Tanaka, H.; Aritsuka, K.; Tachibana, T.; Chuman, H.; Dasgupta, P. K. *Anal. Chim. Acta* **2003**, *499*, 199.

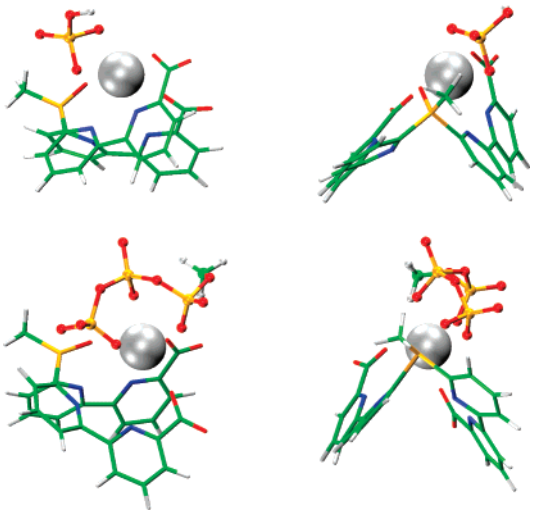

Figure 5. Orthogonal views of the QM-optimized $[Eu\mathbf{L_C}(HPO_4)]^-$ (top) and $[Eu\mathbf{L_C}(MeTP)]^{3-}$ (bottom) ternary complexes.

Table 5. Selected Distances from Europium (Å) in the QM-Optimized $[Eu\mathbf{L_C}(HPO_4)]^-$ and $[Eu\mathbf{L_C}(MeTP)]^{3-}$ Ternary Complexes[a]

		$[Eu\mathbf{L_C}(HPO_4)]^-$ ($[Eu\mathbf{L_B}(HPO_4)]^-$)	$[Eu\mathbf{L_C}MeTP]^{3-}$ ($[Eu\mathbf{L_B}MeTP]^{3-}$)
$\mathbf{L_C}$	$O_{(P=O)}$ (N1 for L^2)	2.492 (3.891)	2.381 (5.029)
		4.542 (2.821)	4.069 (3.338)
		4.238 (2.589)	3.864 (2.814)
		2.792 (4.690)	4.159 (5.671)
		2.638 (4.025)	3.912 (4.546)
		2.350 (2.306)	2.425 (2.424)
		2.342 (2.286)	2.415 (2.436)
	N_2		
	N_3		
	N_4		
	N_5		
	O_1		
	O_2		
HPO_4^{2-}	O_{P1}	2.279 (2.241)	2.314 (2.187)
		2.330 (2.312)	2.332 (2.308)
		4.093 (4.168)	2.336 (2.292)

[a] The corresponding values for complexes with $\mathbf{L_B}$ are given in parentheses.

complexes, and Table 5 summarizes selected optimized distances, also shown in Figure S17 (Supporting Information).

With the $\mathbf{L_C}$ ligand, the $O_{(PO)}$−Eu interactions are found to remain strong in the presence of co-complexed anions (<2.5 Å), in contrast to $\mathbf{L_B}$, where the N_1−Eu bonds were found to lengthen by up to more than 5 Å with the addition of $MeTP^{4-}$. The coordination of europium is thus maintained by the central PO moiety and the two carboxylates. The interaction with the HPO_4^{2-} anion results in a net symmetry disruption (Figure 5). One of the bipyridyl arms remains in close contact, with N_{pyr}−Eu distances of 2.79 and 2.64 Å. The Eu atom sits in the mean plane formed by these two N_{pyr} atoms and the oxygen atoms of the P═O and carboxylate functions. The bidentate HPO_4^{2-} anion is located on one side of this plane, while the second bipyridyl arm faces the anion on the other side, at long N_{pyr}−Eu distances (4.54 and 4.24 Å).

In the optimized $[Eu\mathbf{L_C}(MeTP)]^{3-}$ complex with the $MeTP^{4-}$ anion, the latter is coordinated to europium through the three phosphate groups in a tris-monodentate 1 + 1 + 1 fashion, as in the case of the corresponding $\mathbf{L_B}$ complex. The strong coordination of this anion results in a somewhat decreased coordination strength of the carboxylates, with O−Eu distances reaching ca. 2.42 Å. The four N_{pyr}−Eu distances also increase to ∼4.0 Å; all of the nitrogen lone pairs remain pointing toward the Eu atom (Figure 5). This is in contrast with the $O_{(PO)}$−Eu, distance which shortens to 2.38 Å, similar to the O_{CO2}−Eu distances. The coordinating heteroatoms of $\mathbf{L_C}$ present a bowl-shaped arrangement in which sits the europium atom capped by the $MeTP^{4-}$ anion. Thus, with both co-complexed anions, the $\mathbf{L_C}$ ligand remains firmly anchored to europium by the three O atoms, in deep contrast with $\mathbf{L_B}$ whose N_1 coordination is the first to be disrupted in the presence of competing anions. This is fully consistent with our spectroscopic observations.

Concluding Remarks

The introduction of a phenylphosphine oxide group directly linking the two bipyridyl carboxylate arms induces a pronounced thermodynamic stabilization of the europium complex, as evidenced by the corresponding association constants. In TRIS/$HClO_4$ buffer, a 20-fold increase of the stability is observed ($\Delta \log \beta_{11} = 1.3$) for the coordination of $\mathbf{L_C}$ compared to that of $\mathbf{L_B}$. This stabilization is principally the result of the stronger coordination of the phosphine oxide of $\mathbf{L_C}$ compared to that of the tertiary amine of $\mathbf{L_B}$. A second stabilizing factor comes from the decrease of the conformational freedom of the bipyridyl subunits in $\mathbf{L_C}$, leading to a smaller entropic cost for coordination.[38] For free ligands $\mathbf{L_B}$ or $\mathbf{L_C}$, dipole repulsions lead to a trans arrangement of the central coordinating atom (N_1 in $\mathbf{L_B}$ and $O_{P=O}$ in $\mathbf{L_C}$) and the adjacent N_{pyr} nitrogen atom. The coordination of these atoms to europium to form a five-membered chelate requires a reorganization and rotation around only the P−C_{pyr} bonds in $\mathbf{L_C}$, whereas in $\mathbf{L_B}$ both the N−$C(H_2)$ and $C(H_2)$−C_{pyr} bonds can rotate, resulting in a higher freedom of motion.

The $[Eu\mathbf{L_C}]^+$ complex strongly interacts with various anions (such as ADP^{3-}, ATP^{4-}, and HPO_4^{2-}), as detected by changes in the absorption or luminescence spectra. It is surmised that the stripping of water molecules by the incoming anion in the first coordination sphere of europium accounts for the increase in luminescence lifetimes.

While essential for working with luminescent lanthanide complexes at low concentrations (micro- to nanomolar), the use of ligand $\mathbf{L_C}$ carrying a P═O anchor ensures a marked increase of the complex stability, compared to ligand $\mathbf{L_B}$ bearing a ^{n}BuN fragment. Further interactions with incoming anions remain significant, as shown by the conditional association constants of anions with the complex (log $K_{Eu\mathbf{L_C}(ATP)} = 5.5 \pm 0.2$). However, it is worth noting that the perturbation of the absorption spectrum used as a signature of anion complexation is a more subtle process induced by smoother changes in the coordination mode of $\mathbf{L_C}$.[39] The

(38) (a) Martell, A. E.; Hancock, R. D.; Motekaitis, R. J. *Coord. Chem. Rev.* **1994**, *133*, 39. (b) Hancock, R. D.; Martell, A. E. *Chem. Rev.* **1989**, *89*, 1875.

sensing of anions by the lanthanide complexes of ligands $\mathbf{L_B}$ and $\mathbf{L_C}$ in water results from the delicate balance of the intrinsic stability of the complex and the sequential competitive binding of the incoming anion.

The subtle equilibrium between high stability and tunable coordination may be obtained by engineering less symmetrical ligands endowed with a strongly coordinating part, ensuring stability, and a more weakly coordinating antenna unit, whose binding to the cation is highly sensitive to the presence of incoming anions. Our efforts are currently directed toward the synthesis of such ligands. Because very few systems are indeed functional for the detection of ATP in water and little is known about the mechanism involved in the sensing process, these results highlight the importance of changes in the molecular structure of the ligand upon recognition of the anion.

Experimental Section

Theoretical Methods for QM Calculations. All compounds were fully optimized at the density functional (DFT) level of theory using the B3LYP hybrid functional. The 46 core and $4f^6$ electrons of europium are described by a quasirelativistic effective core potential (ECP) of the Stuttgart group.[40] For the valence orbitals, the affiliated (7s6p5d)/[5s4p3d] basis set was used, enhanced by an additional single f function with an exponent optimized by Frenking et al.[41] The other atoms H, C, N, O, P, and Cl were described by the standard 6-31G* basis set. All calculations have been carried out with Gaussian98.[42] Because of computer time limitations, the butyl chain of $\mathbf{L_B}$, the phenyl rings of $\mathbf{L_C}$, and the ribonucleotide part of AMP, ADP, and ATP were modeled by a methyl group.

Synthesis of the Complexes. Starting Materials and General Procedures. Solvents and reagents were of analytical grade and were used as received. ^{1}H NMR (200.1 and 400.13 MHz) and ^{31}P NMR (161.9 MHz) spectra were recorded on Bruker AC200 and AMX400 spectrometers, using perdeuterated solvents as internal standards. FT-IR spectra were obtained from KBr pellets on a Nicolet 210 spectrometer. Fast-atom bombardment (FAB, positive mode) mass spectra were recorded using *m*-nitrobenzyl alcohol as a matrix. The synthesis of ligand $\mathbf{L_C}$ is given in the Supporting Information.

Preparation of the Complexes. General Procedure. A solution of $LnCl_3 \cdot 6H_2O$ (60 μmol) in MeOH (20 mL) was added to a solution of $\mathbf{L_C}H_2 \cdot 2HCl \cdot H_2O$ (38 mg, 60 μmol) in MeOH and H_2O (10 mL). The resulting mixture was agitated for 3h at 70 °C. Et_3N (33 μL, 240 μmol) was added, and the solution was further agitated for 2 h at room temperature, before the solvent was evaporated. The solid was triturated with Et_2O and dried under vacuum to produce $[Ln\mathbf{L_C}(H_2O)Cl] \cdot xH_2O$.

$[EuL_CCl(H_2O)]$, $x = 3$. Yield: 77%. Yellow crystalline solid. IR (cm^{-1}): 1632 (s, $\nu_{C=O}$), 1593 (s, $\nu_{C=C,C=N}$), 1571 (s, $\nu_{C=C,C=N}$), 1453 (m, $\nu_{C=C}$), 1368 (s, $\nu_{CO_2^-}$), 1256 (m, ν_{C-O}), 1186 (m, $\nu_{P=O}$), 1136 (w), 1015 (w), 810 (w), 776 (s, ν_{CH}). MS (FAB^+): *m*/*z* 671.1 (85%), 673.1 ($[Eu\mathbf{L_C} - Cl]^+$, 100%). Anal. Calcd for $C_{28}H_{17}N_4O_5PEuCl \cdot 4H_2O$: C, 43.12; H, 3.213 N, 7.18. Found: C, 42.90; H, 3.07; N, 7.01

$[TbL_CCl(H_2O)]$, $x = 2$. Yield: 96%. Yellow crystalline product. IR (solid, cm^{-1}): 1628 (s, $\nu_{C=O}$), 1594 (s, $\nu_{C=C,C=N}$), 1571 (s, $\nu_{C=C,C=N}$), 1454 (m, $\nu_{C=C}$), 1368 (s, $\nu_{CO_2^-}$), 1257 (m, ν_{C-O}), 1187 (m, $\nu_{P=O}$), 1168 (m), 1154 (m, $\nu_{P=O}$), 1135 (m), 1084 (m), 1017 (w), 812 (w), 776 (s, ν_{CH}) cm^{-1}. MS (FAB^+): *m*/*z* 679.2 ($[Tb\mathbf{L_C} - Cl]^+$, 100%), 715.3 ($[Tb\mathbf{L_C}Cl + H]^+$, 30%). Anal. Calcd for $C_{28}H_{17}N_4O_5PTbCl \cdot 3H_2O$: C 43.74, H 3.02, N 7.29. Found: C 43.60, H 2.74, N 6.95.

Spectrophotometric Measurements. Analytical grade solvents and chemicals were used without further purification. The purity of the adenosine derivatives was checked by ^{31}P NMR (less than 5% impurity). The TRIS/HCl and $HClO_4$ buffer solutions 0.01 M in water were obtained by acidification of the 0.01 M TRIS solution with the corresponding acid, using Fixanal pH 7.00 as the reference solution. Stock solutions of lanthanides were prepared from the corresponding chloride salts, $LnCl_3 \cdot 6H_2O$ (Ln = Eu and Tb). UV−vis absorption spectra were measured on a Uvikon 933 (Kontron Instrument, Milano, Italy) spectrometer using quartz Suprasil cells with a 1 cm path length. Spectrophotometric titrations were performed on the same apparatus. In a typical experiment for ligands titrations as a function of added lanthanide, 5×10^{-5} M ligand solution in buffered 0.01 M TRIS solution (pH 7.0) was titrated with $LnCl_3 \cdot 6H_2O$ solutions at different concentrations (from 2 to 5×10^{-4} M). After the addition of each aliquot, the absorption spectrum of the solution was recorded. The same conditions were used for the titrations as a function of added anions. The factor analysis and mathematical treatment of the spectrophotometric data were performed with the SPECFIT program.[29] In the case of titration with anions, the model consisted in the fitting of the equilibria 1 and 4, to which was added protonation equilibria corresponding to the acido−basic reactions potentially occurring around pH 7.0 ($5.0 < pK_a < 9.0$). Typical examples are protonation of AMP^{2-} ($pK = 6.21$),[10d] ADP^{3-} ($pK = 6.40$),[10d] ATP^{4-} ($pK = 6.47$),[10d] and HPO_4^{2-} ($pK = 7.2$).[37] The calculated constants are averaged values of at least two individual titration experiments given with the average deviation.

Luminescence Measurements. Low-resolution luminescence measurements (spectra) were recorded on a Perkin-Elmer LS50B spectrometer. Emission and excitation spectra were measured in a 1 cm path length quartz Suprasil cell at room temperature (25 °C) and corrected for the instrumental function. Luminescence quantum yields were determined in the phosphorescence mode with a 0 μs delay time and a 20 ms integration windows, using $[Ru(bipy)_3]Cl_2$ in non degassed water ($\phi = 2.8\%$)[43] or Rhodamine 6G in ethanol ($\phi = 88\%$)[44] as references. When necessary, a 350 nm cutoff filter was used to eliminate the second generation harmonic artifacts. Phosphorescence lifetimes (τ) were measured in solutions on a PTI

(39) A lanthanide complex working on the sequential competitive binding mode similar to $[Eu\mathbf{L_B}]^+$, but in the visible part of the spectrum, has been recently reported, see: Li, S.-H.; Yuan, W.-T.; Zhu, C.-Q.; Xu, J.-G. *Anal. Biochem.* **2004**, *331*, 235.

(40) Dolg, M.; Stoll, H.; Savin, A.; Preuss, H. *Theor. Chim. Acta* **1989**, *75*, 173−194.

(41) Ehlers, A. W.; Böhme, M.; Dapprich, S.; Gobbi, A.; Höllwarth, A.; Jonas, V.; Köhler, K. F.; Stegmann, R.; Veldkamp, A.; Frenking, G. *Chem. Phys. Lett.* **1993**, *208*, 111.

(42) Frisch, M. J.; Trucks, G. W.; Schlegel, H. B.; Scuseria, G. E.; Robb, M. A.; Cheeseman, J. R.; Zakrzewski, V. G.; Montgomery, J. A., Jr.; Stratmann, R. E.; Burant, J. C.; Dapprich, S.; Millam, J. M.; Daniels, A. D.; Kudin, K. N.; Strain, M. C.; Farkas, O.; Tomasi, J.; Barone, V.; Cossi, M.; Cammi, R.; Mennucci, B.; Pomelli, C.; Adamo, C.; Clifford, S.; Ochterski, J.; Petersson, G. A.; Ayala, P. Y.; Cui, Q.; Morokuma, K.; Malick, D. K.; Rabuck, A. D.; Raghavachari, K.; Foresman, J. B.; Cioslowski, J.; Ortiz, J. V.; Stefanov, B. B.; Liu, G.; Liashenko, A.; Piskorz, P.; Komaromi, I.; Gomperts, R.; Martin, R. L.; Fox, D. J.; Keith, T.; Al-Laham, M. A.; Peng, C. Y.; Nanayakkara, A.; Gonzalez, C.; Challacombe, M.; Gill, P. M. W.; Johnson, B.; Chen, W.; Wong, M. W.; Andres, J. L.; Gonzalez, C.; Head-Gordon, M.; Replogle, E. S.; Pople, J. A. *Gaussian 98*, revision A.5; Gaussian, Inc.: Pittsburgh, PA, 1998.

(43) Nakamura, K. *Bull. Chem. Soc. Jpn.* **1982**, *55*, 2697.

(44) Olmsted, J., III. *J. Phys. Chem.* **1979**, *83*, 2581.

QuantaMaster spectrophotometer. They were obtained by monitoring the decay at the maxima of the emission spectra upon UV-excitation, using 1000 channels on period ranging from at least 5τ. The decays, monoexponential or biexponential, were analyzed with the software implemented method.

Acknowledgment. This work is supported by the French CNRS. We thanks Michel Schmitt for recording the ^{31}P NMR spectra. We are embedded to Professor Michael Chetcuti from the Laboratoire de Chimie Organominérale Appliquée at the ECPM for critical comments and helpful discussions.

Supporting Information Available: Synthesis and full characterization of $\mathbf{L_C}$, QM-optimized structures and distances of $[Eu\mathbf{L_B}X(H_2O)_n]^+$ (Figures S1 and S2, $X = NO_3^-$, HPO_4^{2-}, $MeDP^{3-}$, $MeTP;^{4-}$ $n = 0$ or 2) and $[Eu\mathbf{L_C}X]^+$ (Figures S17, $X = HPO_4^{2-}$ and $MeTP^{4-}$) structures, UV−vis spectrophotometric titration data for complexation of $\mathbf{L_C}$ by $EuCl_3 \cdot 6H_2O$ in TRIS/HCl and $HClO_4$ (Figures S3−S6) and for the association of ADP^{3-}, ATP^{4-}, and HPO_4^{2-} to $[Eu\mathbf{L_C}]^+$ (Figures S7−S15), normalized metal-centered emission intensity for the titration of $[Eu\mathbf{L_C}]^+$ by anions (Figure S16), and the luminescence lifetime evolution as a function of added anions (Table T1−T4, $X^- = NO_3^-$, ADP^{3-}, $MeTP^{4-}$, and HPO_4^{2-}, respectively). This material is available free of charge via the Internet at http://pubs.acs.org.

IC051033O